Energy 34 (2009) 1207–1214

Contents lists available at ScienceDirect

Energy

journal homepage: www.elsevier.com/locate/energy

Improvement of electrical arc furnace operation with an appropriate model

Labar Hocine*, Djeghader Yacine, Bounaya Kamel, Kelaiaia Mounia Samira

Department of Electrical Engineering, Faculty of Engineering Sciences, University of Annaba, B.P. 12, Annaba 23000, Algeria

ARTICLE INFO

Article history:
Received 12 October 2008
Received in revised form
28 February 2009
Accepted 5 March 2009
Available online 12 June 2009

Keywords:
Modelling
Electric arc furnace
Power quality
Flicker

ABSTRACT

Electrical arc furnaces are commonly employed in industry to produce molten steel by melting iron and scrap steel. Furnace control is a necessary operation for production optimization. The principal parameters to be controlled are: maximum productivity requirements, minimum power off time, good power quality and safety. The aim of this study is to achieve all these objectives. Hence, because of the stochastic and dynamic behaviour of the arc during the melting process, a proposed model is checked with measurements at an industrial electrical arc furnace. How electrodes position and transformer taps can affect *X* and *R* arc function are discussed in detail. This new operating strategy has been determined taking into account Flicker, melting stages and electrode positions. It is shown that optimum efficiency can be reached by the integration of the proposed model in regulation loop.

1. Introduction

Nonlinear loads are the principal cause of power quality problems [1] including voltage dips, harmonic distortion and Flicker [2–4]. An electrical arc furnace (EAF) is the worst nonlinear load type, because of the chaotic nature of arc impedance [5] as its conductivity is determined from temperature and pressure [6].

Irregularity in the voltage wave forms is caused by abrupt initiation [7] and interruption of current which provides a source of harmonic currents (Fig. 1). Thus voltage and current waves deviate considerably from a symmetrical sinusoidal form.

The increase in iron demand such as in vehicle industries encourages steel makers to invest more in metal recycling using electrical or chemical furnaces. It is known that electrical arc furnaces are used to provide high-quality steels from a raw material of steel scrap.

A typical furnace is shown in Fig 2. It consists of a refractory lined shell, a removable roof, three graphite electrodes, held in clamps at the end of a supporting arm, passing through openings in the furnace roof. Electrical power is supplied to the electrodes by an adjustable AC voltage tap transformer and the heat is generated by electric arcs between electrodes. Once a temperature of 1300 °C is reached the metal scrap starts melting (Fig. 3).

The maximum electrical power converted into heat occurs for a particular length of electric arc [8]. Any deviation from this optimum length impairs the power utilization efficiency. The steel load surface is irregular by nature of the scrap and as the melting process begins there is a change in the contours of the surface. Thus, random disturbances in the arc length occur continuously. It is the function of the position control system to respond to such disturbances by moving the electrode to maintain the arc length at its preset value [9].

1.1. Typical EAF process

First we load the furnace with metal scrap, then the electrodes can be lowered within the furnace using a specific regulator and mechanical drive for each electrode. The electrodes are connected to the furnace transformers, which may be rated from 90 to 265 volts, using 9 taps. To achieve meltdown as quickly as possible, one must follow the following stages [10,11].

Stage 1: The current is initiated by lowering the electrodes, just over the metal scrap.
Stage 2: Electrodes bore through the scrap to form a pool of liquid metal.
Stage 3: Electrical arc is lengthened by increasing the voltage to maximum power.
Stage 4: Arc length is changed so that the shorter arc will deliver a higher portion of its heat to the metal below the electrode.
Stage 5: Chemical treatments to improve steel quality are done under low power to maintain the liquid state.
Stage 6: The process is ended and the liquid metal is transferred.

* Corresponding author. Tel./fax: +213 38 875 398.
E-mail address: hocine.labar@univ-annaba.org (L. Hocine).

0360-5442/$ – see front matter © 2009 Elsevier Ltd. All rights reserved.
doi:10.1016/j.energy.2009.03.003

Nomenclature

P_{EAF}	total active power
P_{arc}	arc active power
Q_{EAF}	total reactive power
Q_{arc}	arc reactive power
Q^L_{EAF}	arc inductive reactive power
Q^C_{arc}	arc capacitive reactive power
X_{arc}	arc reactive impedance
X^L_{arc}	arc electromagnetic impedance
X^C_{arc}	arc electrostatic impedance
EAF	electric arc furnace
n	number of measurements
d	distance between electrodes and scrap
I_e	electrode current
U_1	electrode voltage

2. Model description

To operate the EAF considered in this study, an AC current is applied to graphite electrodes. It requires about 520 kWh/ton (Fig. 4a). All the processes of the electrical arc furnace (Appendix AAppendix A) can be summarized in Fig. 5 [12]. We have recorded 32 measurements for each parameter in 9 transformer taps (Fig. 4b). The operation of the electrical arc furnace is subjected to two main constraints, namely normal power and rated current. Fig. 5 shows the various limits of operation for each voltage tap. The control of the process by the rated current does not protect it sufficiently, since the absorbed power can largely exceed the capability of the furnace transformer. On the other hand, the control by the rating power offers a better protection for the furnace.

3. Instruments and error analysis

Currents, tensions and power measurements are done with standard precision instruments "model Goerz AE 111 S" connected to the secondary EAF transformer:

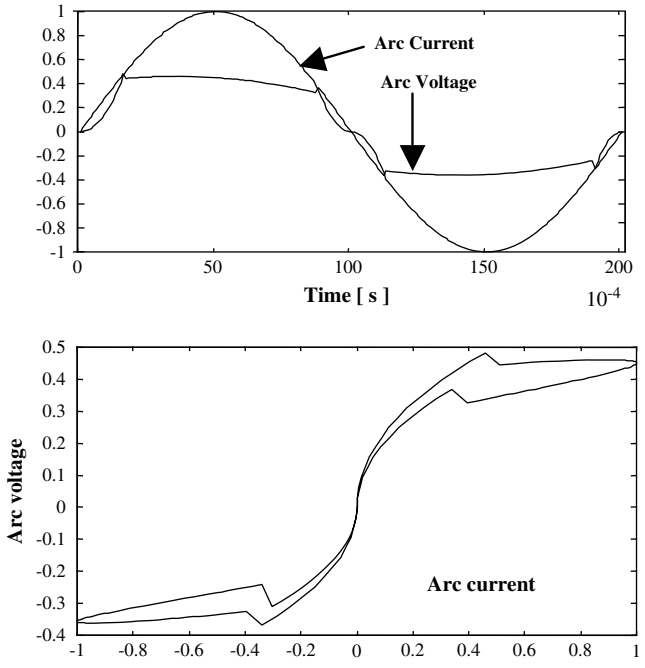

Fig. 1. Temporal and [IV] representation of electric arc current and voltage.

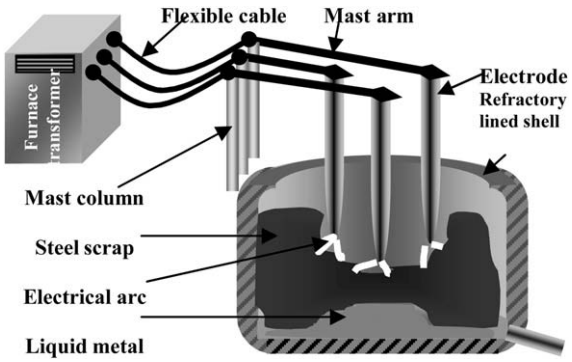

Fig. 2. Typical electrical arc furnace.

- Ampere-meter: 0–6 A, class 0.5
- Voltmeter: 90–265 V, class 0.5
- Wattmeter: 5 A, 130 V, class 0.5
- Transformer of current: 5–10–25–50/5 A, class 0.2

If one tests the instruments in the case of normal operation, under the effect of the electric arc, they can be distorted by the chaotic nature of the arc. For this reason, the tests are made in short-circuit mode, when immersing electrodes directly in the liquid steel (Table 1). For each case, phase current, lines to ground voltage and phase power are recorded (Table 2).

The maximum deviation of the impedance, resistance and inductance calculated for each test (Table 3) are respectively 2.89%, 3.73% and 2.98%. However, the melting process is supplied in three-phase current (with electrodes a, b and c) and the maximum errors are respectively 2.15%, 2.90% and 2.21%. Although these values are reached under extreme conditions, in the case of the EAF, they are of a very good precision because of the nonlinear and chaotic characteristics of the electric arcs. In normal operating mode, large deviations occur.

4. Measured parameters analysis

There are several working models of the electric arc furnace from the thermal point of view [13]. Our proposal is based on a modelling of the electrical parameters. The EAF is modelled together with the neighbouring network [14].The circuit equation of the furnace transformer up to the end of electrodes can be written as follows:

$$E_{tr} = \sqrt{3}Z_1 I_e + U_1 \quad (1)$$

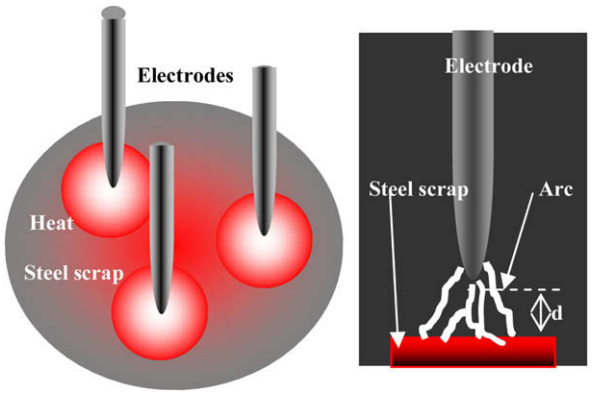

Fig. 3. Heat conversion by electric arc.

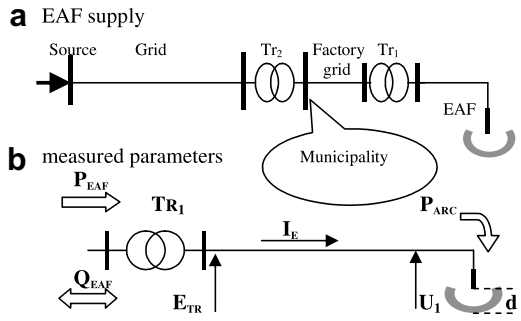

Fig. 4. Studied model.

where Z_1 is the impedance of EAF transformer with the flexible cable.

Then,

$$Z_1 = \frac{[E_{tr} - U_1]}{\sqrt{3}I_e} = \frac{\Delta U_1}{\sqrt{3}I_e} \tag{2}$$

$$Z_1 = \sqrt{R_1^2(I_2, T) + X_1^2(T)} \tag{3}$$

where

$$R_1 = \frac{P_{\mathrm{EAF}} - P_{\mathrm{arc}}}{3I_e^2} \tag{4a}$$

In this case, R_1 is measured using the equation:

$$R_1 = R_{\mathrm{tr}} + R_{\mathrm{flexible\ cable}} \tag{4b}$$

So, from Eqs. (2–4) one can deduce Eq. (5)

$$X_1 = \frac{1}{\sqrt{3}I_e}\sqrt{\Delta U_1^2 - \frac{[P_{\mathrm{EAF}} - P_{\mathrm{arc}}]^2}{3I_e^2}} \tag{5}$$

Fig. 6a and b show the variations of resistance R_1 and inductance X_1 of the transformer with the flexible cable which supplies the electrodes.

Indeed, for the various tests carried out:

- R_1 has a Gaussian distribution (Fig. 6a); this is due to the combined effect of applied current and elapsed time. The dispersion is more important at low voltage, because metal takes more time to melt, which leads to overheating of the transformer winding and the flexible cable.
- As inductance X_1 is the consequence of electromagnetic fields, which are weakened with the temperature increase, it gives a decaying exponential variation (Fig. 6b).

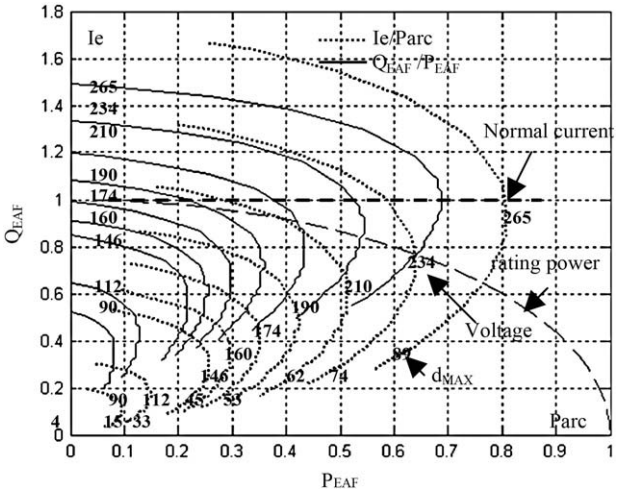

Fig. 5. EAF electro energetic process.

Table 1
Test cases.

Test	Electrode a	Electrode b	Electrode c
a–b	On	On	Off
a–c	On	Off	On
b–c	Off	On	On
a–b–c	On	On	On

In order to reduce this parametric dispersion, we propose to ameliorate cooling by forced ventilation of transformer windings and increase water flow that crosses the flexible cables.

Subsequently using all measured parameters, we try to define the electric arc characteristics. Because an electric arc creates heat conversion, the model must present arc resistance as in Eq. (6):

$$R_{\mathrm{arc}} = \frac{P_{\mathrm{arc}}}{3I_e^2} \tag{6}$$

The unwired conduction of the electric arccontributes to conduction of reactive parameters Eq. (7) created between the electrodes and the scrap.

$$Q_{\mathrm{EAF}} = Q_{\mathrm{arc}} + \Delta Q \tag{7}$$

$$Q_{\mathrm{arc}} = Q_{\mathrm{EAF}} - 3I_e^2 X_1 \tag{8}$$

$$X_{\mathrm{arc}} = \frac{Q_{\mathrm{arc}}}{3I_e^2} \tag{9}$$

Following to this assumption and the measurements analysis, an empirical model is proposed (Eqs. (10) and (11)), with the variables, voltage taps (U) and the distance (d) between the electrodes and the scrap. The novelty of this approach gives 2 degrees of freedom to the model compared to fixed values under estimated parameters proposed by Tongxin et al. [15].

$$R_{\mathrm{arc}} = A_R(u) \times e^{\alpha(u)d} \tag{10}$$

where

$$A_R = \frac{\left[0.7 \times (U-210)^2 + 1.7\right]}{50^2} \times 10^{-3};$$

$$\alpha = 0.097e^{0.011(90-U)} - \frac{1.7}{(U-112)^2+80} + \frac{100}{(U-360)^2+50}$$

$$X_{arc} = A_X(u)d^2 + B_X(u) \tag{11}$$

where

Table 2
Measurement results.

Test	Electrode currents, kA			Electrode voltages, V			Active power, MW		
	a	b	c	a	b	c	a	b	c
a–b	23.38	23.38	0	114.1	113.7	234.9	0.35	0.35	0
a–c	23.25	0	23.25	113.5	242.1	115.3	0.35	0	0.35
b–c	0	22.63	22.72	241.9	114.3	116.6	0	0.31	0.31
a–b–c	25.51	25.69	25.49	130.4	130.4	130.4	0.4	0.4	0.4

Table 3
Calculation of electrical parameters.

Test	Impedance Z, mΩ			Resistance R, mΩ			Inductance X, mΩ		
	a	b	c	a	b	c	a	b	c
a–b	4.8802	4.5631	–	0.6403	0.6403	–	4.8381	4.8208	–
	−2.55%	−2.89%	–	2.58%	2.58%	–	−2.63%	−2.98%	–
a–c	4.8817	–	4.9591	0.6475	–	0.6475	4.8386	–	4.9167
	−2.52%	–	−0.97%	3.73%	–	3.73%	−2.62%	–	−1.05%
b–c	–	5.0508	5.1320	–	0.6053	0.6005	–	5.0144	5.0968
	–	0.86%	2.48%	–	−3.02%	−3.79%	–	0.92%	2.56%
a–b–c	5.1117	5.0759	5.1157	0.6147	0.6061	0.6156	5.0746	5.0396	5.0786
	2.07%	1.36%	2.15%	−1.53%	−2.90%	−1.37%	2.13%	1.43%	2.21%
Average		5.0078			0.6242			4.9687	

$$A_X = 1.05 \times 10^{-3} \times e^{0.075(90-U)}$$

and

$$B_X = \frac{3.14 \times U}{153} - 3 \times 10^{-3} \times e^{0.075(90-U)}$$

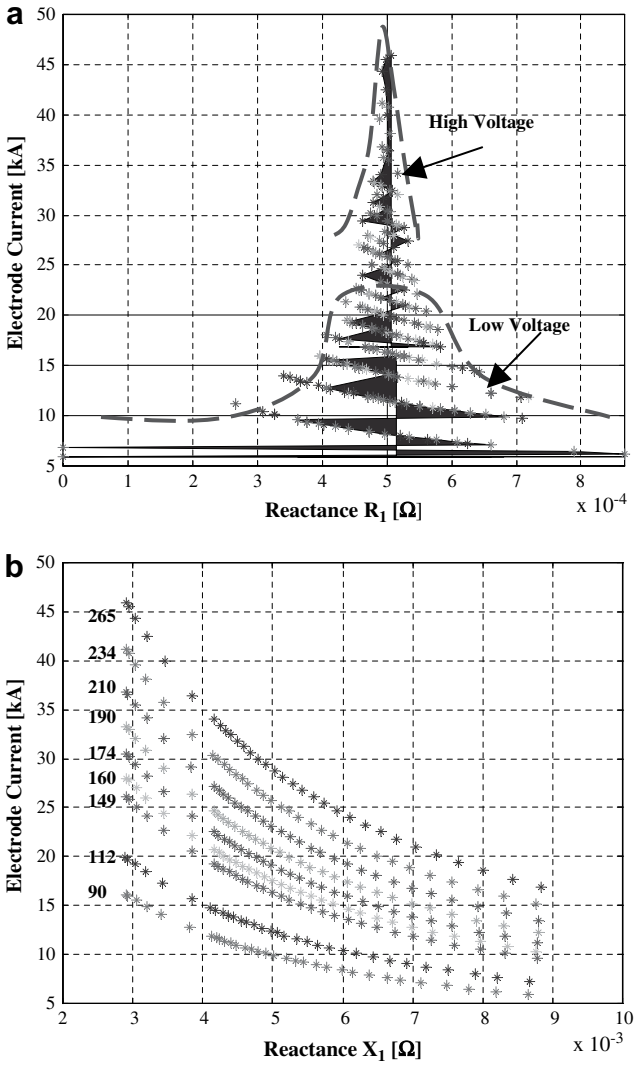

Fig. 6. Calculation of Z_1 form the 9×32 measurements.

In the operating zone, the arc impedance decreases with the increase of voltage and increases with the distance between electrodes and metal. Fig. 7 shows the error of the model compared to the measured parameters. The analysis concludes that for high voltages and short arc distance, the electrostatic field created between the electrode and the metal is more important as the electromagnetic fields give to the arc a capacitive character defined by the negative values of X_{arc} (Fig. 7b). For this purpose, we propose a model of electric arc as shown in Fig. 8.

It has been advanced that an electric arc presents two types of field (Eq. (12)), where each field is characterized by its own parameters, Eqs. (13) and (14):

$$Q_{arc} = Q^L_{arc} + Q^C_{arc} \tag{12}$$

$$Q^L_{arc} = K_L d \tag{13}$$

$$Q^C_{arc} = -K_C / d \tag{14}$$

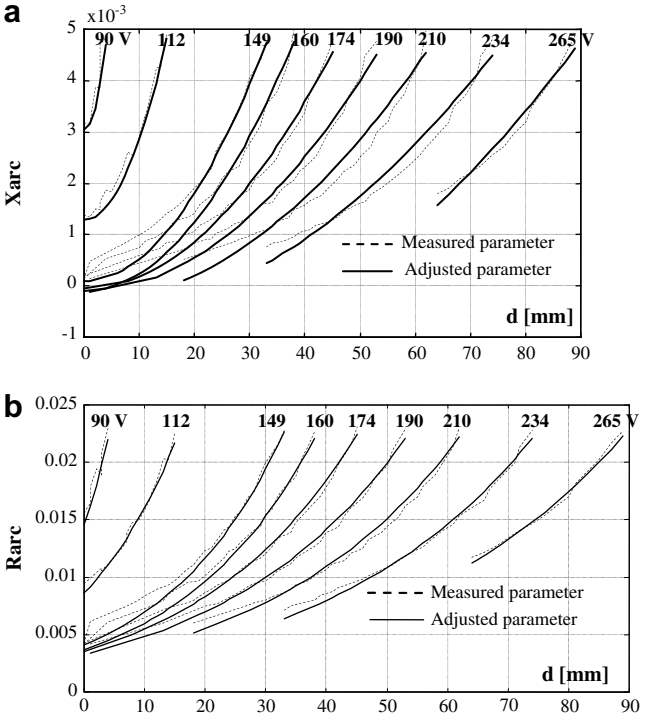

Fig. 7. Variation of electric arc impedance.

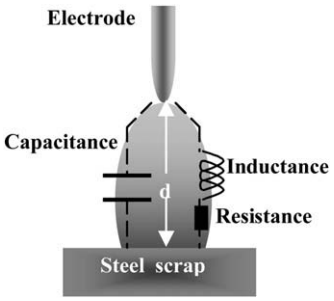

Fig. 8. Electric arc model.

Introducing relations in Eqs. (13) and (14) into Eq. (12), we obtain the expression defined by Eq. (15):

$$Q_{\text{arc}} = \frac{\left[K_L d^2 - K_C\right]}{d} \tag{15}$$

$$K_L(n) = \frac{Q_{\text{arc}}(n+1)\times d(n+1) - Q_{\text{arc}}(n)\times d(n)}{d^2(n+1) - d^2(n)} \tag{16}$$

$$K_C(n) = K_L(n)d^2(n+1) - Q_{\text{arc}}(n+1)d(n+1) \tag{17}$$

$$Q^L_{\text{arc}} = K_L \times d = 3 \times X^L_{\text{arc}} \times I_e^2 \Rightarrow X^L_{\text{arc}} = K_L d/3I_e^2 \tag{18}$$

$$Q^C_{\text{arc}} = -K_c/d = -U_1^2/X^C_{\text{arc}} \Rightarrow X^C_{\text{arc}} = U_1^2 \times d/K_c \tag{19}$$

The process can take different positions of electrodes for various voltage taps, so, according to Eqs. (18) and (19), one can estimate the different variation of X^L_{arc} and X^C_{arc} (Fig. 9) for all of the process.

In order to show the importance of furnace model establishment, its behaviour is tested without and then with integration of our suggested model in the regulation loop.

5. Results of simulation

5.1. Error in the model simulation

The differential equations in the simulation are solved by Ode23tb with a scalar relative error tolerance = 10^{-3}, and an absolute error tolerance = 10^{-6} for all components.

The comparison between the real and proposed model shows very close results, but for low voltages, the difference is not negligible (Fig. 10); this mode is used to initiate the electric arc during

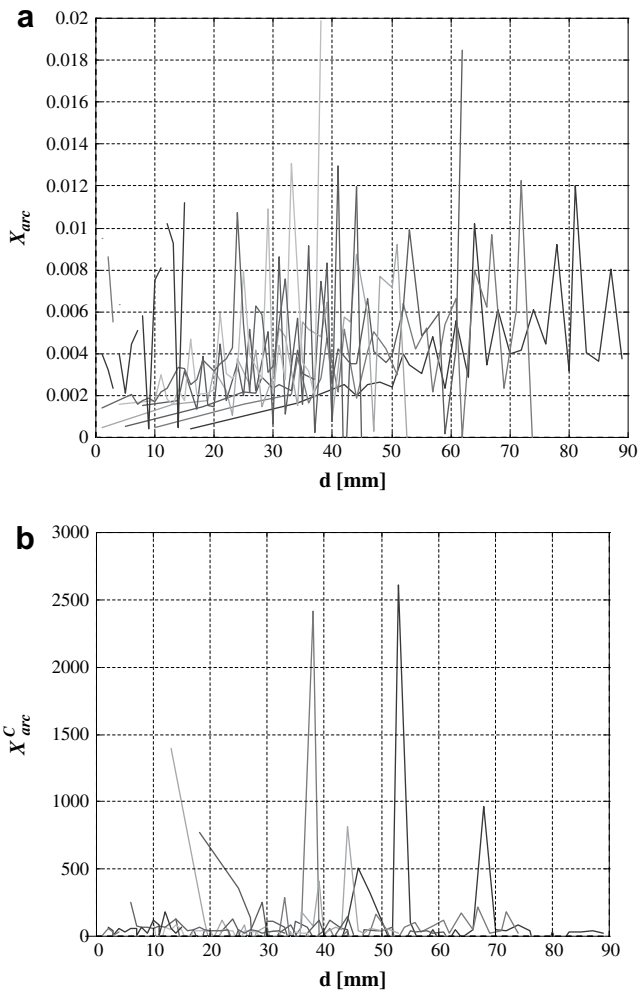

Fig. 9. Calculation of Z_{arc} form the 9×32 measurements.

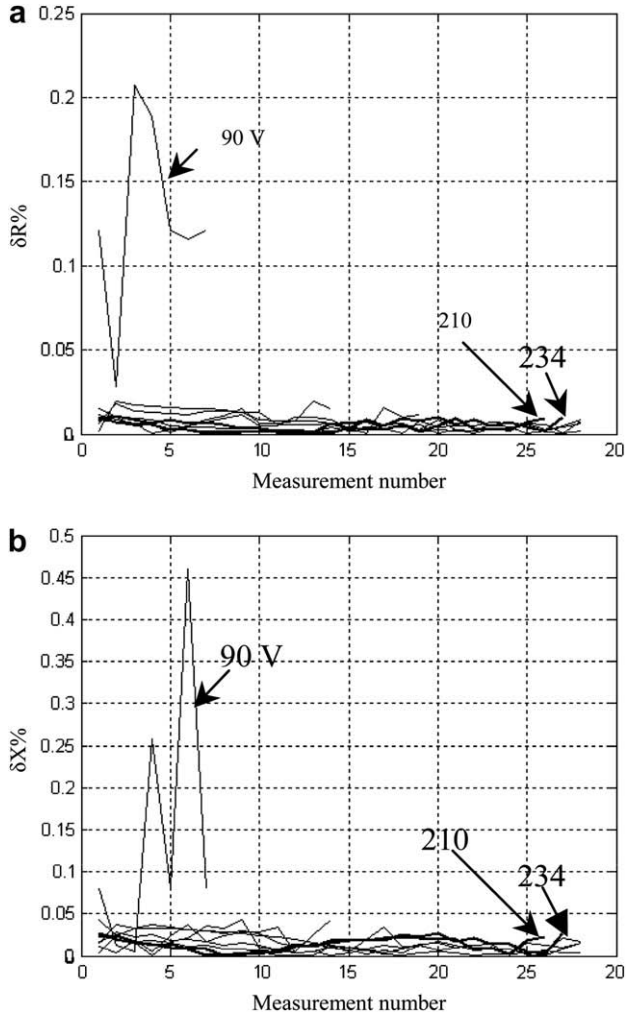

Fig. 10. Comparison of absolute errors between the real and proposed model.

2 min at the latest. Normal working voltages of this electric furnace are 234 and 210 volts, and its maximum errors are respectively for:

- Resistance 0.0107% and 0.0096%
- Inductance 0.0235% and 0.0275%

The global errors (Fig. 10) show that the generalized model proposed in this paper can be implemented in the regulation loop of the EAF so as to improve its global operation and management of metal scrap loads.

5.2. Regulation without model

Fig. 11a shows that the acceptable apparent power is largely exceeded, which results in rapid ageing of the electrical power equipment (transformer, circuit breaker, contactor, relay etc.). As for the power, the current presents dangerous overcurrents (Fig. 11b), compared to its rated value; this reveals other electric arcs which may attack the internal wall of the furnace (refractory lined shell), in addition to the wear of electrode heads. The other consequence is the voltage drop at the main bus bars of the furnace (Flicker).

5.3. Regulation with model

Fig. 12a shows a better exploitation, with some short and weak overtaking of the furnace power load because of the system inertia which controls the electrodes. The other benefit is the stability in the power arc. Also, the effectiveness of the integration of the model in the regulation loop is achieved by the reduction of Flicker using a very moderate current (Fig. 12b).

All the evoked points have technical advantages. To be accepted in industry the innovative approaches must be subjected to an economical proof [16]. The first obvious economic aspect with this model is an increase in the longevity of electrical and mechanical equipment. The other benefit is shown in Fig. 13 where we make the comparison between the two tests on the electrical power conversion into heat, which gives a possibility of increasing the production up to 30%.

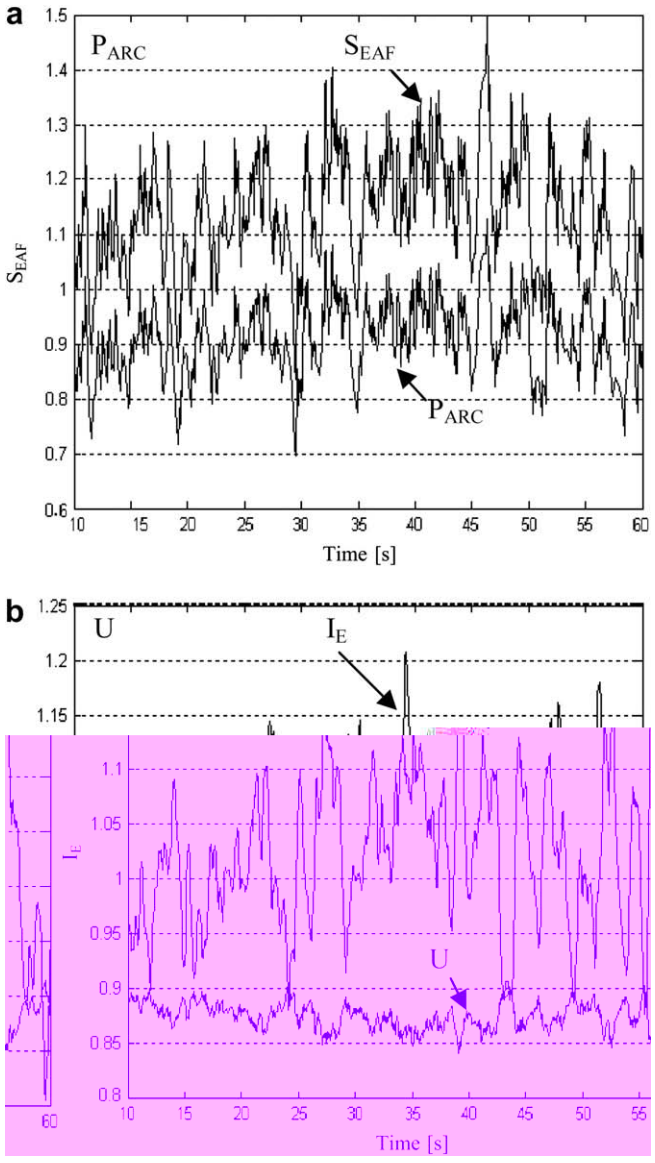

Fig. 11. Test result without model.

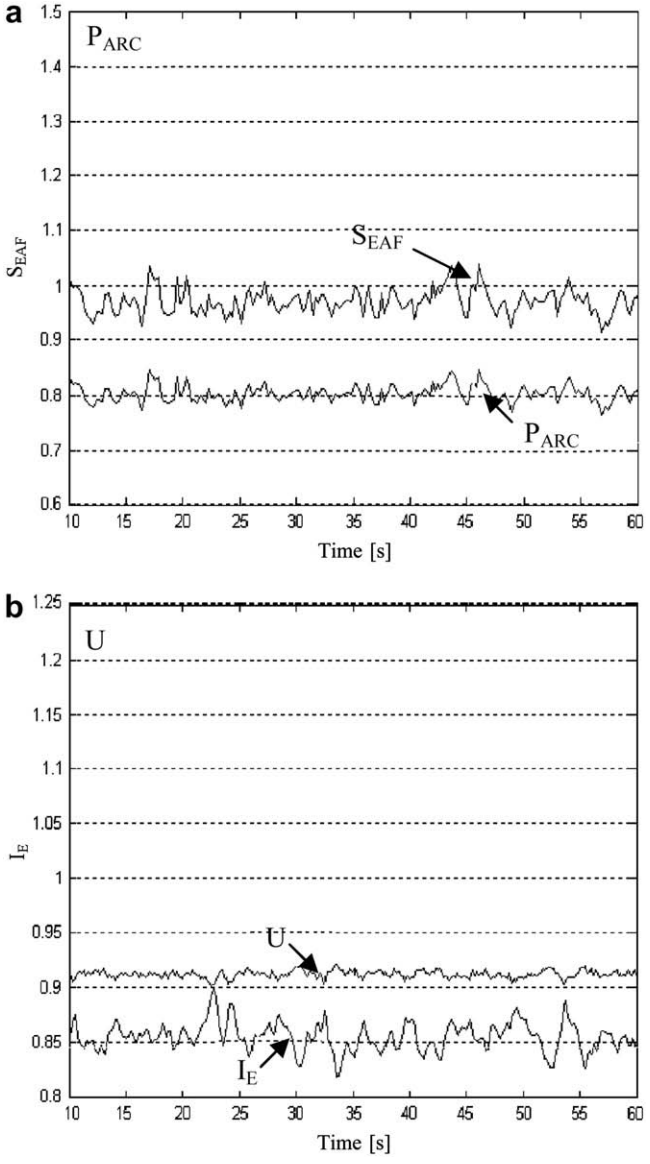

Fig. 12. Test result with model.

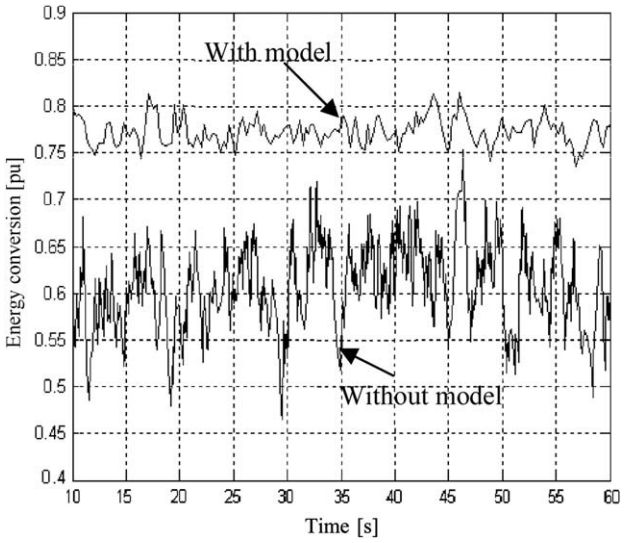

Fig. 13. Coefficient of energy conversion.

Since the furnace is connected to the environment, through an electrical network there could be some pollution (chemical and sonic aspects). During exploitation, it can cause several risks (harmonics propagations, Flicker, voltage collapse, etc.). These disturbances also affect the normal operation of the furnace itself. In order to highlight these disturbances, we show in Fig. 14 the effect of Flicker on the motor which controls the distance between electrodes and metal scrap. This motor is in the neighbourhood of the furnace loading system. So, for the case without integration of the model in the regulation loop, the rotor inflicts very strong oscillations, and on the other hand it becomes more stable in the case of model integration.

The major part of power quality problems occurs in the first and second stage of the melting process, because of the physical movement and the settling of the scrap. It is proposed to substitute the electrical energy by a chemical one [17], like natural gas, and that the EAF be electrically supplied only in stages 3 and 4.

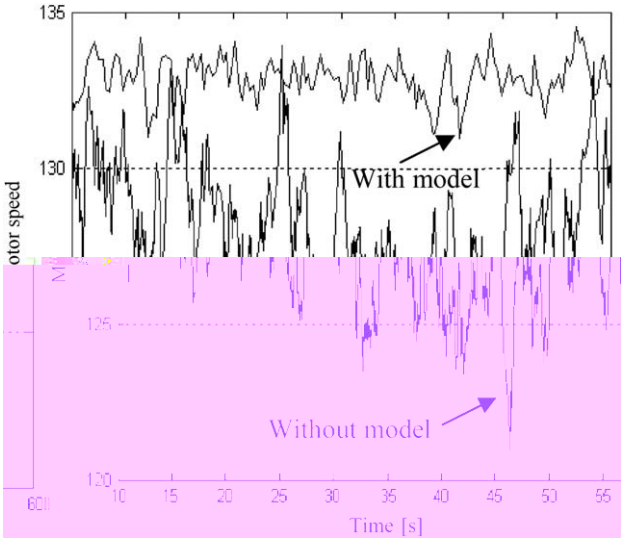

Fig. 14. Effect of power quality disturbance on motor speed of electrodes regulators.

6. Conclusion

This analysis leads to the conclusion that the arc behaves in such a way that all the arc characteristics are controlled by the expansion of the arc, which is the main feature used to physically describe the arc behaviour. Arc expansion is evident from the arc shape, which is the region where conduction of electricity takes place. The arc shape depends on current density, magnetic flux density, electric conductivity, electric potential and temperature. The proposed model reveals a new parameter of the electrical arc furnace, namely the capacitance.

Because of the continuous adjustment of electrode position, the integration of this model in the regulation loop reduces operator actions; thus reduction of human errors due to the visual estimation. Therefore this automation will enable better management of energy. The electrical energy for the same number of tons of treated scrap is reduced by up to 30%.

The empirical relations of furnace capacitance and inductance enable us to:

- Have a good tracking performance
- Reduce the impact to electrical network
- Avoid some dangerous current and voltage oscillations
- Reduce the melting time
- Adjust the three phases into balance effectively
- Have a wide range of controls
- Enhance productivity

The other recommendation to steel makers is to substitute electrical energy for stages 1 and 2 by a chemical one, because of power quality constraint.

Appendix A EAF features

EAF type: 80LHF12.5
Transformer rating: 12.5 [MVA]
Short circuit reactance: 2.9 [mΩ]
Maximum electrode current 30.84 [kA]
Number of voltage taps: 9
Voltage range: [90 V ÷ 265 V]
Primary voltage: 63 [kV]
Weight capacity: 80 t
Temperature gradient: 3 ÷ 4 [°C/min]
Furnace diameter: 2.47 [m]
Electrode diameter: 0.35 [m]
Distance electrode to wall: 0.71 [m]

References

[1] Esmaili M, Shayanfar HA, Jalilian A. Modal analysis of power systems to mitigate harmonic resonance considering load models. Energy 2008;33(9):1361–8.
[2] Ozgun O, Bur A. Development of an arc furnace model for power quality studies. IEEE Power Engineering Soci 1999;6:507–11.
[3] Andrews D, Bishop MT, Witte JF. Harmonic measurements, analysis and power factor correction in a modern steel manufacturing facility. IEEE Transactions on Industry Applications 1996;32(3):617–24.
[4] Routimo M, Salo M, Tuusa H. Comparison of voltage-source and current-source shunt active power filters. PESC 2005 Power Electronics Specialists Conference IEEE 2005:2571–7.
[5] Carpinelli G, Iacovone F, Russo A, Varilone P. Chaos-based modelling of DC arc furnaces for power quality issues. IEEE Transactions on Power Delivery 2004;19(4):1869–76.
[6] Sakulin M. Simulation of electric arcs in melting furnaces. BNCE 1982; Electro heat for Metals Conference, Cambridge, p. 1.4
[7] Emanuel AE, Orr JA. An improved method of simulation of the arc voltage–current characteristic. International Conference on Harmonics and Quality of Power, Orlando, Florida; 2000; p. 148-150

[8] Cano Plata EA, Tacca HE. Arc furnace modelling in ATPEMTP. IPST 2005; International Conference on Power Systems Transients, Montréal, Canada
[9] Boulet B, Lalli G, Ajersch M. Modelling and control of an electric arc furnace. American Control Conference, Denver, Colorado, 2003; p. 3060-3064
[10] Zheng T, Makram EB. An adaptive arc furnace model. IEEE Transactions on Power Delivery 2000;15(3):931–9.
[11] Collantes-Bellido R, Gomez T. Identification and modelling of a three phase arc furnace for voltage disturbance simulation. IEEE 1997;12: 1812–7. T.P.D.
[12] Timm K. Circle diagram of AC-Furnaces. Electrical Engineering of Arc Furnaces Symposium. Germany 2005:18–21.
[13] Kirschen M, Velikorodov V, Pfeifer H. Mathematical modelling of heat transfer in deducting plants and comparison to off-gas measurements at electric arc furnaces. Energy 2006;31(14):2926–39.
[14] Schau H, Stade D. Mathematical modelling of three-phase arc furnaces. ICHPS II 1994. Bologna: IEEE; 1994. 422–428.
[15] Zhang T, Makram EB. An adaptive arc furnace model. IEEE Trans. Power Delivery 2000;15:931–9.
[16] Zhang J, Wang G. Energy saving technologies and productive efficiency in the Chinese iron and steel sector. Energy 2008;33(4):525–37.
[17] Ziebik A, Lampert K, Szega M. Energy analysis of a blast-furnace system operating with the Corex process and CO_2 removal. Energy 2008;33(2):199–205.